The Cooperative Voltage Sensor Motion that Gates a Potassium Channel

Medha Pathak,[1] Lisa Kurtz,[2] Francesco Tombola,[2] and Ehud Isacoff[1,2]

[1]Biophysics Graduate Group, and [2]Department of Molecular and Cell Biology, University of California, Berkeley, Berkeley, CA 94720

ABSTRACT The four arginine-rich S4 helices of a voltage-gated channel move outward through the membrane in response to depolarization, opening and closing gates to generate a transient ionic current. Coupling of voltage sensing to gating was originally thought to operate with the S4s moving independently from an inward/resting to an outward/activated conformation, so that when all four S4s are activated, the gates are driven to open or closed. However, S4 has also been found to influence the cooperative opening step (Smith-Maxwell et al., 1998a), suggesting a more complex mechanism of coupling. Using fluorescence to monitor structural rearrangements in a Shaker channel mutant, the ILT channel (Ledwell and Aldrich, 1999), that energetically isolates the steps of activation from the cooperative opening step, we find that opening is accompanied by a previously unknown and cooperative movement of S4. This gating motion of S4 appears to be coupled to the internal S6 gate and to two forms of slow inactivation. Our results suggest that S4 plays a direct role in gating. While large transmembrane rearrangements of S4 may be required to unlock the gating machinery, as proposed before, it appears to be the gating motion of S4 that drives the gates to open and close.

KEY WORDS: potassium channel • S4 • gating • cooperativity • coupling

INTRODUCTION

Voltage-gated potassium channels consist of four identical subunits, each subunit made up of six α-helical transmembrane (TM) segments (S1–S6) and a pore loop (Yellen, 1998). Segments S5 and S6 and the pore loop of each subunit assemble to form the channel's pore. Ion selectivity is conferred by a series of amino acids in the pore loop called the selectivity filter. Two gates in the channel's pore regulate permeability: the internal S6 gate, which is formed by an inverted teepee-like arrangement of the S6 helices, and the slow inactivation gate, which resides in the selectivity filter. The conformation of these gates is controlled by the channel's voltage-sensing domains, which are formed by segments S1–S4 of each subunit. The S4 segment, which has several basic residues, is the primary voltage sensor of the channel (Yang and Horn, 1995; Aggarwal and MacKinnon, 1996; Larsson et al., 1996; Seoh et al., 1996; Yang et al., 1996; Baker et al., 1998; Wang et al., 1999; Ahern and Horn, 2004).

The motion of the four S4s through the membrane electric field mediates voltage sensing. In response to membrane depolarization, gating charge is displaced in a series of steps in each subunit, carrying the equivalent of approximately three charges across the membrane per subunit (Schoppa et al., 1992; Stefani et al., 1994; Zagotta et al., 1994a,b; Baker et al., 1998; Schoppa and Sigworth, 1998a,b,c; Cha et al., 1999; Glauner et al., 1999; Lecar et al., 2003). The gating charge displacement is due to sequential outward motions of S4 that appear to displace it by a total of ~13 Å axially relative to its surround, and rotate it by as much as a half turn (Aggarwal and MacKinnon, 1996; Larsson et al., 1996; Mannuzzu et al., 1996; Yang et al., 1996; Baker et al., 1998; Cha et al., 1999; Glauner et al., 1999; Wang et al., 1999; Gandhi and Isacoff, 2002; Lecar et al., 2003). S4 motion controls the conformation of the S6 gate by an unknown mechanism to open a permeation pathway from the cytoplasm through the selectivity filter to the outside of the cell (Armstrong, 1969; Liu et al., 1997). The major gating charge displacing steps of voltage sensing are referred to as "activation" in this paper, and the subsequent conformational changes that result in an open S6 gate are referred to as "opening."

In related, nonvoltage sensitive 2-TM potassium channels, the internal gate opens by a bending at a conserved glycine of the inner helix TM2, which is homologous to S6 (Jiang et al., 2002a). This rearrangement is thought to be elicited by a centrifugal pull on the internal end of TM2 by ligand binding in the COOH-terminal cytoplasmic domain. The TM2/S6 bending motion appears to be accompanied by a lateral motion of the internal end of the surrounding TM1/S5 helix. Opening of voltage-gated K^+ channels may occur when S5 is pulled laterally by S4 via the S4–S5 linker allowing S6 to bend (Isacoff et al., 1991; Holmgren et al., 1996; Sanguinetti and Xu, 1999; Jiang et al., 2002a,b, 2003a,b). It is not known how the voltage-sens-

Correspondence to Ehud Y. Isacoff: eisacoff@socrates.berkeley.edu

Abbreviations used in this paper: 4-AP, 4-aminopyridine; HP, holding potential; TGM, tetraglycine maleimide; TEVC, two-electrode voltage clamp; TM, transmembrane; TMRM, tetramethylrhodamine; WT, wild type.

J. Gen. Physiol. © The Rockefeller University Press • 0022-1295/2005/01/57/13 $8.00
Volume 125 January 2005 57–69
http://www.jgp.org/cgi/doi/10.1085/jgp.200409197

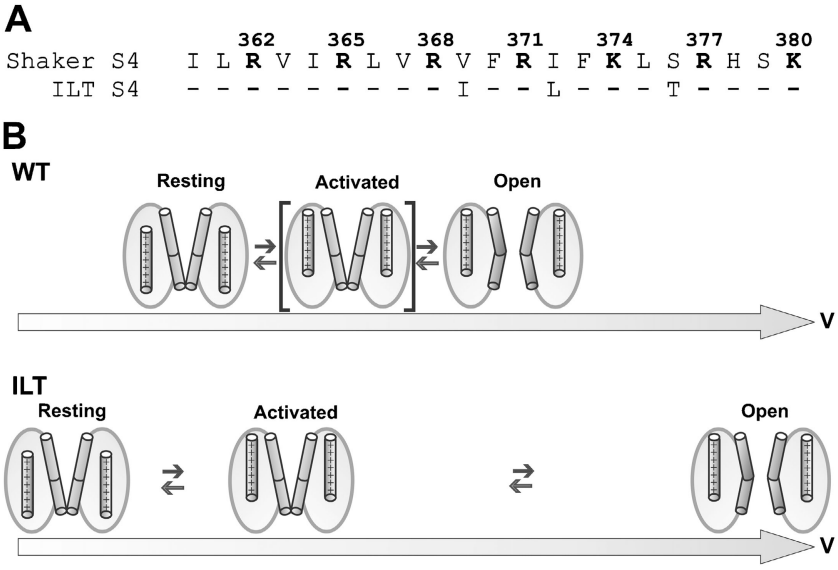

FIGURE 1. The ILT mutant channel. (A) The S4 sequence for Shaker and for the ILT mutant channel. Charged residues are denoted in bold and numbered. (B) Cartoon illustrating activation and opening in WT and ILT channels. Only two subunits of the channel are shown, with the positively charged helix S4 and the S6 helix. The long gray arrow represents a voltage axis ranging from −150 to 200 mV. In the WT channel (top), activation and opening are tightly coupled and the activated state is short-lived (denoted by a bracket around the activated state). In the ILT channel (bottom), activation is negatively shifted, whereas opening is positively shifted. Cartoon based on results from Ledwell and Aldrich (1999).

ing motions of S4 control the S6 gate. Furthermore, opening itself is voltage dependent (Schoppa and Sigworth, 1998c; Smith-Maxwell et al., 1998b; Ledwell and Aldrich, 1999), and the source of this voltage dependence is not known (Patlak, 1999).

In wild-type (WT) Shaker channels, the rates and voltage dependence of both, the activation and opening transitions are similar, making it difficult to study opening in isolation from the previous voltage-sensing steps. In the ILT mutant of the Shaker channel the final step of channel opening is energetically isolated from the preceding voltage-sensing steps (Fig. 1; Ledwell and Aldrich, 1999). This mutant, formed from three conservative substitutions in the Shaker S4 (V369I, I372L, and S376T) has been extensively characterized by Aldrich and coworkers (Smith-Maxwell et al., 1998b; Ledwell and Aldrich, 1999). Several lines of evidence from their work suggest that the ILT mutations do not alter the basic mechanism of gating. First, each of the three ILT mutations is a conservative amino acid substitution that does not alter the chemistry of the side chain. Individual substitutions of any one of the ILT mutations cause only modest change in gating behavior compared with WT, suggesting that each of the point mutations is well tolerated by the protein structure. Second, ILT ionic currents in the higher end of the voltage range of opening show a Shaker-like sigmoidal delay, indicating that the ILT channel also goes through several intermediate states before opening. Third, gating currents recorded from the ILT channel in a voltage range where the channels do not open are very similar to Shaker gating currents in kinetics, suggesting that the two channels go through similar intermediate states. Fourth, ILT behavior could be described by modifying the parameters of a kinetic model developed for the Shaker channel. The ILT channel thus makes an excellent system in which to study the molecular rearrangements involved in the final steps of channel opening following activation. The key features of ILT behavior are: (a) the ionic currents are slow and monoexponential over a large voltage range, indicating that a single transition in the gating pathway is made rate limiting, (b) the voltage dependence of gating charge movement (Q–V curve) is shifted to negative voltages, whereas that of channel opening (G–V curve) is shifted to positive voltages so that activation and opening occur over different voltage ranges, and (c) while most of the gating charge moves during activation, a small component ($\sim$1.8 e_0) moves with opening. We took advantage of the fact that activation and opening in ILT channels occur over different, nonoverlapping voltage ranges to focus separately on either the major gating charge moving steps of activation or on the opening process.

We monitored the motion of S4 in ILT channels using the environmentally sensitive fluorophore tetramethylrhodamine (TMRM), which reports on local protein motions (Mannuzzu et al., 1996; Gandhi et al., 2000). We find that S4 moves not only during activation, but also over the voltage range of opening of the S6 gate and of two forms of slow inactivation gating. Single subunit fluorescence measurements from heterotetrameric channels show that this gating motion of S4 is cooperative across the four subunits. We propose that the gating motion of S4 underlies the voltage dependence of the opening step and is the only motion of S4 that exerts force on the channel's gates.

MATERIALS AND METHODS

Molecular Biology

The ILT construct (V369I, I372L, S376T in ShB Δ6–46) was provided by R. Aldrich (Stanford University, Stanford, CA). Experi-

ments with WT were performed on Shaker H4 (Δ6–46) channels, which differ in amino acid sequence from ShB (Δ6–46) in nonconserved regions but are electrophysiologically indistinguishable from ShB (Δ6–46). For fluorescence experiments, all constructs were made nonconducting with the W434F mutation (Perozo et al., 1993). Point mutations were introduced with QuickChange (Stratagene) and were confirmed by DNA sequencing. RNA was transcribed using T7 *mMessage mMachine* (Ambion). For experiments that required the NH_2-terminal fast inactivation ball, it was subcloned from Shaker B into the ILT construct between the BamHI and the SacII restriction sites. This construct was designated as "ILT + ball."

Channel Expression and Fluorescence Labeling

For all of the fluorescence experiments, 50 nl of mRNA (at 1 ng/nl) was injected into *Xenopus laevis* oocytes. For the fluorescence cooperativity experiments, in order to create heterotetrameric channels of the desired stoichiometry, a 1.5:8.5 ratio of RNA encoding the labelable subunit (i.e., containing an engineered cysteine at site 359) to RNA encoding the unlabelable subunit was injected into *Xenopus* oocytes, as described previously (Mannuzzu and Isacoff, 2000). The concentration of each RNA species was checked before injection by spectroscopy and gel electrophoresis. Assuming free association between subunits, at this ratio, most (62%) of the fluorescence signal would originate from channels with only one fluorophore binding subunit.

In all of the fluorescence experiments, oocytes were incubated at 12°C in ND96 (96 mM NaCl, 2 mM KCl, 1.8 mM $CaCl_2$, 1 mM $MgCl_2$, 5 mM HEPES, pH 7.6) for several hours after injection, and then native cysteines were blocked by incubation for 20 min at room temperature in tetraglycine maleimide (TGM). The oocytes were then washed and incubated at 18°C in ND96 for 2–8 d before recording. On the recording day, the oocytes were labeled with TMRM on ice in the dark in a high potassium solution (92 mM KCl, 0.75 mM $CaCl_2$, 1 mM $MgCl_2$, 10 mM HEPES, pH 7.5). Depending on the site, incubation was done with 5–50 μM TMRM for 25–50 min. After labeling, the oocytes were washed and kept in ND96 at 10°C in the dark until being voltage clamped. This procedure is as previously described (Mannuzzu et al., 1996) except that the TGM block was done soon after RNA injection, before any channels arrived on the surface, thus ensuring that no channels would be labeled with TGM.

Electrophysiology

Voltage clamp fluorometry was performed as previously described (Mannuzzu et al., 1996). Cell membrane potential was controlled by the two-electrode voltage-clamp technique using a Dagan CA-1 amplifier (Dagan Corporation). Fluorescence measurements were performed on a Carl Zeiss MicroImaging, Inc. IM35 microscope using a 20× 0.75 numerical aperture fluorescence objective and a 100 W mercury arc lamp, with a Hamamatsu HC120–05 photomultiplier tube. The photomultiplier and Uniblitz shutter (Vincent Associates) signals were controlled by the Digidata-1200 board and PClamp8 software package (Axon Instruments). Fluorescence signals were filtered with a Chroma High Q TRITC filter, low-pass filtered at 3 kHz with an 8-pole Bessel filter and digitized at 10 kHz. Recording solutions contained 80 mM NaMES, 2 mM KMES, 2 mM CaMES, 10 mM HEPES, and 28 mM MEA (to prevent bleaching), pH 7.5.

Gating current recordings were done in the two-electrode voltage clamp configuration (TEVC), 5–7 d after RNA injection. For all gating current measurements, the holding potential (HP) was −80 mV, with a 50-ms prestep to −120 mV followed by a voltage step to the specified potential. The gating charge was calculated by integrating the Off gating current. We did not attempt to measure the charge moved during opening in ILT channels due to contaminating endogenous currents observed in TEVC. Macropatch recordings from excised inside-out patches on conducting channels (W434) were done 1–3 d after injection using an Axopatch 200A amplifier. Pipettes had a resistance in the range of 0.7–1.3 MΩ. Pipette solution was composed of 140 mM KCl, 6 mM $MgCl_2$, 10 mM HEPES, pH 7.1, and bath solution of 140 mM KCl, 11 mM EGTA, 10 mM HEPES, pH 7.2 with NMDG.

Data Analysis

Data analysis was performed using Clampfit 8 (Axon Instruments) and Origin 6.0 (Microcal). Charge–voltage (Q–V) relations were constructed from integrated "off" gating currents. Fluorescence–voltage (F–V) relations were constructed from the steady-state amplitudes of fluorescence changes, and normalized to the amplitudes of single (for all WT data) or double Boltzmann fits (for 359C ILT and 358C ILT). For 351C ILT, 356C ILT, and 361C ILT, the data were normalized to the minimum and maximum data points. Conductance–voltage (G–V) relations were constructed from the amplitude of tail currents that followed test voltage steps to open the channels. The data were fit to Boltzmann functions using Origin 6.0 (Microcal). Error bars show standard error of the mean unless otherwise noted. For measuring the voltage dependence of P-type inactivation, where long protocols had to be used in the inside-out patch configuration, the amplitude of peak current in the test pulse was adjusted to account for rundown of channels from the patch. The rundown of current was assumed to be a linear function of time. Ionic current in response to a 200-mV voltage step was measured at the beginning ($I_{initial}$) and end (I_{final}) of the protocol, and the current in each test step (Fig. 6 A) was increased by a factor: $t_{step}((I_{initial} - I_{final})/(t_{initial} - t_{final}))$.

RESULTS

S6 Gate Is Closed in the Activated State

As a channel opens from the resting state, it goes through several intermediate states, some of which are capable of passing ions (Chapman et al., 1997; Zheng and Sigworth, 1998; Zheng et al., 2001). These subconductance states are short-lived and have been proposed to reveal the sequential opening of a gate in the selectivity filter of each subunit (Zheng et al., 2001). The pore gate appears to be coupled to the S6 gate of the channel so that channel opening involves both gates (Flynn and Zagotta, 2001). We wondered whether in the ILT channel there is an uncoupling between S4 and the pore gate, i.e., whether in the activated state (at 0 mV) the ILT channel has an open S6 gate but a closed pore gate that keeps the channel nonconducting. We addressed this question by probing the open/closed conformation of the S6 gate in the activated state of the ILT channel using the NH_2-terminal fast inactivation ball, which can bind to internal mouth of the pore and block conduction only when the S6 gate is open (Armstrong, 1969; Fig. 2 A).

We cloned the ball from ShB into the ILT channel and confirmed that the ILT+ball channel undergoes fast inactivation (Fig. 2 B). Steady-state prepulse inactiva-

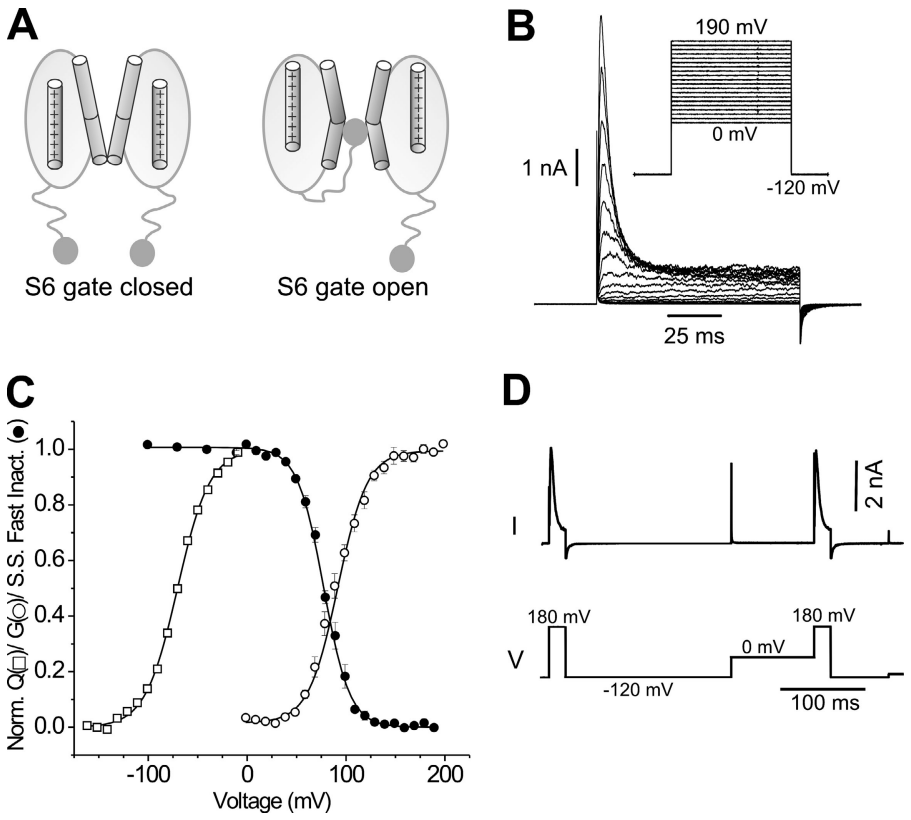

FIGURE 2. S6 gate in ILT channels is closed in the activated conformation. (A) Cartoon showing that the NH_2-terminal ball can block the channel only when the S6 gate is open. (B) ILT+ball channels show fast inactivation in excised inside-out macropatches. Inset shows voltage protocol used, HP = −100 mV. (C) Fast inactivation in ILT+ball channels takes place over the voltage range of opening, not activation. Steady-state (S.S) prepulse fast inactivation for ILT+ball channels (closed circles) measured from peak amplitude of current during a 20-ms test pulse to +180 mV following a 100-ms voltage step to the specified potential, HP = −100 mV with a 50-ms prestep to −120 mV. G–V from ILT channels (open circles) constructed as described in MATERIALS AND METHODS, Q–V (open squares) measured from integrated OFF gating currents of ILT W434F channels. Solid lines are Boltzmann fits to the data. Fit parameters: ILT Q–V, $V_{1/2}$ = −70.4 mV, slope factor = 16.3 mV, representative of n = 8; ILT+ball prepulse inactivation curve, $V_{1/2}$ = +77.3 mV, slope factor = 13.3, average of data from 11 patches; ILT G–V, $V_{1/2}$ = +91.8 mV, slope factor = 14.9, average of data from 8 patches. (D) Two voltage pulses to +180 mV, from a prestep to −120 mV and from an ensuing prestep to 0 mV, yield currents with similar amplitude in ILT+ball channels. Representative trace of n = 6.

tion (Fig. 2 C, filled circles) does not occur over the voltage range of channel activation (Q–V; Fig. 2 C, square symbols), but takes place over the voltage range of opening (G–V, Fig. 2 C, open circles). Similarly, a comparison of peak current amplitudes evoked by a test pulse to +180 mV from two different presteps revealed no inactivation at the negative voltages of activation: no significant difference in peak current amplitude was observed for test pulses following presteps to −120 mV (where channels are at rest) or 0 mV (where channels are activated) (Fig. 2 D). These observations indicate that the ball does not have access to its binding site when the ILT channel is activated. Thus, the S6 gate is closed in the activated ILT channel. The effect of the ILT mutations therefore appears to be on the coupling between the activation motion of S4 and the S6 gate, supporting earlier interpretation (Webster et al., 2004).

S4 Moves Along with Opening

Even though activation and opening are energetically separated in ILT channels, opening continues to be weakly voltage dependent, carrying ∼1.8 e_0, i.e., ∼13% of the total charge moved by the channel (Ledwell and Aldrich, 1999), similar to the amount estimated for the cooperative opening steps of WT channels (Schoppa and Sigworth, 1998c). The molecular origin of this gating charge movement is not known. We asked whether S4 motion might underlie this gating charge of the opening step. We approached this question by using fluorescence to detect S4 motion over the voltage range of ILT ionic currents.

TMRM was covalently attached to a cysteine engineered at site 359 of the S4 segment, and the fluorescence intensity change was measured over a voltage range that spans ILT activation and opening, i.e., from −150 to +200 mV (Fig. 3 A). For 359C WT channels in the nonconducting (W434F) background, the fluorescence intensity changed between −150 and +20 mV and showed no further change with increasing depolarization. TMRM fluorescence intensity measured from 359C ILT W434F channels changed throughout the entire voltage range, and had two prominent components. The first component of the fluorescence intensity change plotted as a function of voltage (F–V) spanned the voltage range of −150 to 0 mV, where ILT channels activate, and the second component occurred over 0 to 200 mV, where ILT channels open. The F–V relation for 359C ILT channels was fit by a double Boltzmann function. To confirm that the first and second F–V components of 359C ILT W434F reported on acti-

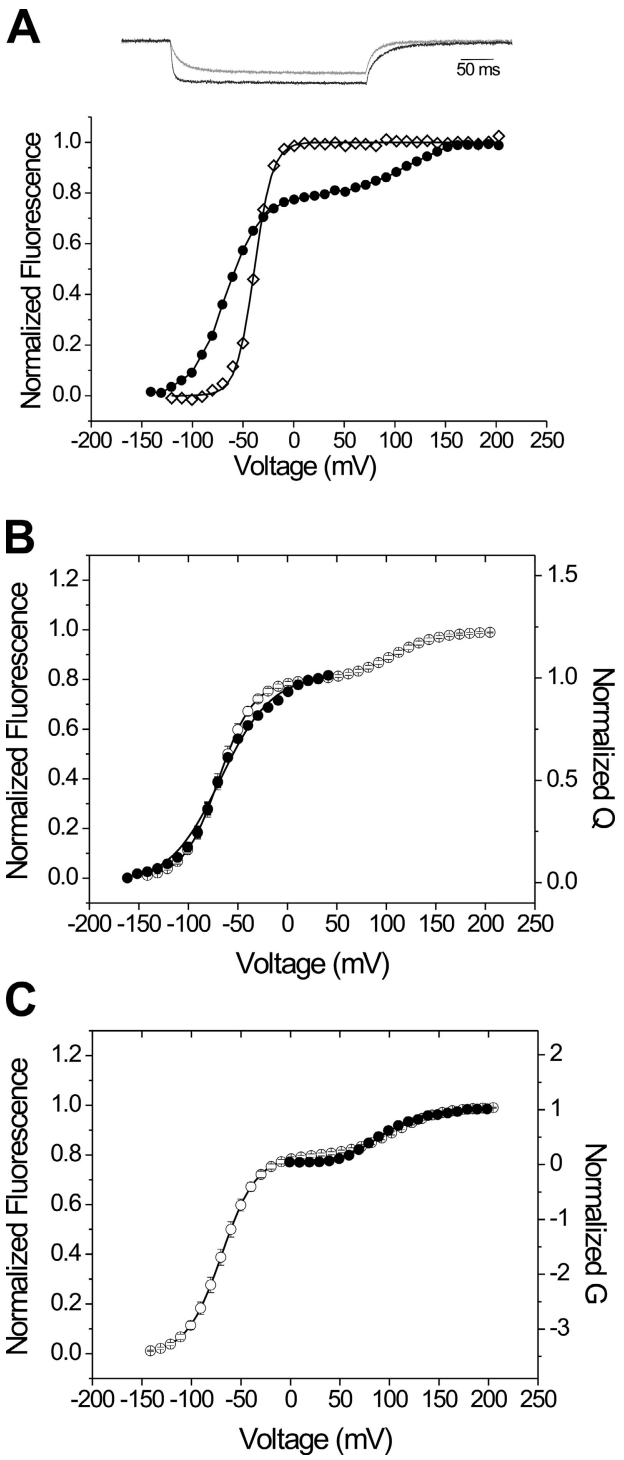

FIGURE 3. S4 attached TMRM senses protein motion over voltage range of ILT channel opening. (A) Normalized steady-state F–V for 359C WT W434F (open diamonds) and for 359C ILT W434F (closed circles). F–Vs are normalized to the amplitude of single Boltzmann fit for 359C WT and a double Boltzmann fit for 359C ILT (fits are solid lines). Fit parameters: 359C WT W434F $V_{1/2}$ = −43.8 mV, slope factor = 7.3, representative of n = 13; 359C ILT W434F $V1_{1/2}$ = −66.8 mV, slope factor = 17.2, $V2_{1/2}$ = +105.6 mV, slope factor = 24.1, representative of n = 18. Traces on top show the fluorescence intensity change evoked from a prestep of −120 mV to voltage step to 0 mV (gray) or 180 mV (black) for 359C ILT W434F channels. HP = −80 mV. (B and C) Superimposition of the Q–V from 359C-TMRM ILT W434F channels (B, filled circles), and the G–V from 359C-TMRM ILT channels (C, filled circles) with the F–V from 359C-TMRM ILT W434F channels (open circles). F–V and Q–V measured in two-electrode voltage clamp configuration, and G–V measured from excised inside-out macropatches. Each data point is a mean of n = 5 for the Q–V, n = 9 for G–V, and n = 9 for F–V. Solid lines are Boltzmann fits to the data. Fit parameters: Q–V $V_{1/2}$ = −67.3 mV, slope factor = 25.8; G–V $V_{1/2}$ = 94.3 mV, slope factor = 22; F–V double Boltzmann fit parameters: $V1_{1/2}$ = −69.5 mV, slope factor = 17.6, $V2_{1/2}$ = +105.1 mV, slope factor = 23.3.

vation and opening respectively, we measured the Q–V from TMRM-labeled 359C ILT W434F channels and the G–V from conducting TMRM-labeled 359C ILT channels. The measured Q–V approximates the first Boltzmann component of the F–V for 359C ILT W434F (Fig. 3 B), and the measured G–V approximates the second Boltzmann component of the F–V (Fig. 3 C). Thus, the two phases of fluorescence intensity change of TMRM in 359C ILT suggest that, separately from its activation motion, S4 has an additional rearrangement over the voltage range of channel opening. However, we considered the possibility that TMRM at site 359 may also sense rearrangements in other nearby parts of the channel, such as the pore domain (Cha and Bezanilla, 1998; Loots and Isacoff, 2000). To determine if the opening rearrangement directly involved S4, we performed a fluorescence scan involving sites at the outer end of S4 and in the proximal S3–S4 linker. We reasoned that if TMRM at site 359 sensed the opening rearrangement that occurs elsewhere in the protein, then it would not sense the opening rearrangement when attached at positions that point in other directions. We examined the fluorescence of TMRM attached at four other nearby sites: 351, 356, 358, and 361. TMRM at all of the sites changed fluorescence over the voltage ranges of both activation and opening in ILT channels (Fig. 4). The fluorophore attached to the same sites in WT channels did not change fluorescence over the voltage range of ILT opening. The fluorescence reports differed from site to site in ILT channels (Fig. 4), indicating that TMRM senses distinct environments at these positions and supporting the idea that as a group, the positions will reflect the motion of S4 relative to its surround. Since we detect fluorescence changes associated with the final gating motion of S4 at each of the five sites at and near the outer end of the ILT channel's S4, we conclude that either there is a motion of S4 during opening, or that there is a motion of the entire region surrounding S4. Functionally, this is the same thing. What matters is not S4's position relative to some absolute reference, but relative to the protein surrounding it.

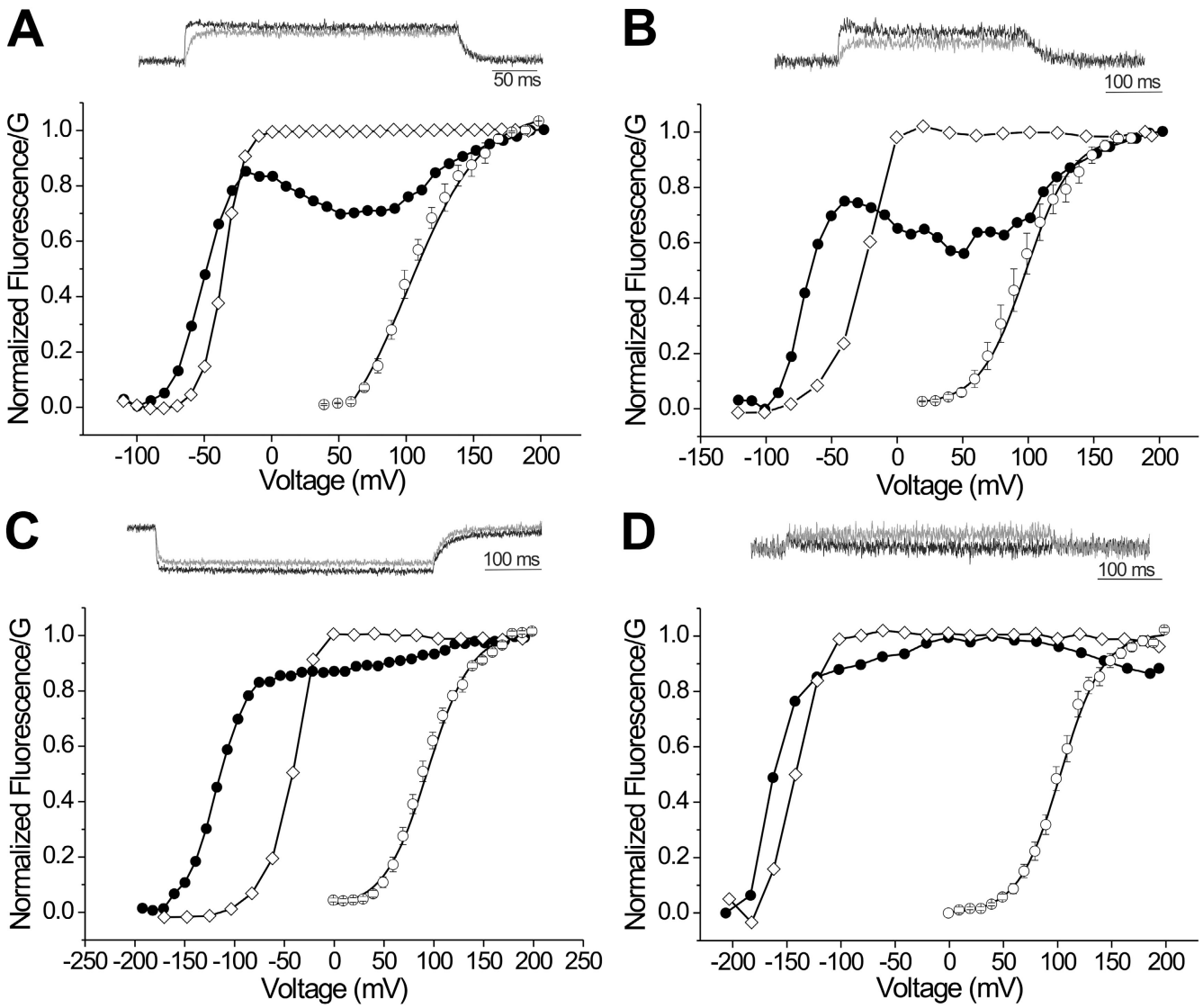

FIGURE 4. Opening rearrangement sensed at four sites in S4 and proximal S3–S4 linker. Steady-state fluorescence behavior of TMRM attached to sites 351C (A), 356C (B), 358C (C), and 361C (D). Each panel shows the F–Vs for TMRM attached to the specified site in the WT W434F background (open diamonds) and in the ILT W434F background (filled circles). Open circles show G–Vs measured from excised inside-out macropatches for ILT channels labeled with TMRM at the specified site. Traces on top of each graph show the fluorescence intensity change in response to a step to 0 mV (gray) and 180 mV (black) from a prestep to −120 mV in the ILT W434F background. HP = −80 mV. Different amounts of separation between the WT and ILT F–Vs at the four positions likely reflect different impacts on gating of the cysteine mutation and TMRM labeling. F–Vs are representative of $n = 7$ for 351C ILT, $n = 6$ for 351C WT, $n = 3$ for 356C ILT, $n = 10$ for 356C WT, $n = 3$ for 358C ILT, $n = 6$ for 358C WT, $n = 6$ for 361C ILT, $n = 4$ for 361C WT. Fit parameters for G–Vs: 351C ILT $V_{1/2}$ = 113.6 mV, slope factor = 21.2, $n = 3$; 356C ILT $V_{1/2}$ = 96.1 mV, slope factor = 20.5, $n = 6$; 358C ILT $V_{1/2}$ = 94.3 mV, slope factor = 22.0 mV, $n = 6$; 361C ILT $V_{1/2}$ = 102.9 mV, slope factor = 19.5, $n = 9$.

To test the interpretation that S4 motion accompanies opening, we used a different specific assay that interferes with opening. We reasoned that if an S4 motion were tightly associated with the opening rearrangement, then a selective inhibition of the opening transition would be expected to also block this motion of S4. We tested this prediction by examining the effect of 4-aminopyridine (4-AP), which has been shown to block the gating charge movement associated with the opening step of the channel (McCormack et al., 1994; Loboda and Armstrong, 2001). We measured fluorescence from TMRM attached to 359C ILT W434F channels before and after application of 2 mM 4-AP to the bath solution (Fig. 5). While the fluorescence change accompanying activation persisted in the presence of 4-AP, the fluorescence change over the voltage range of ILT opening was abolished. This finding supports the conclusion that S4 motion accompanies channel opening. This gating motion of S4 seems likely to underlie the voltage dependence of opening.

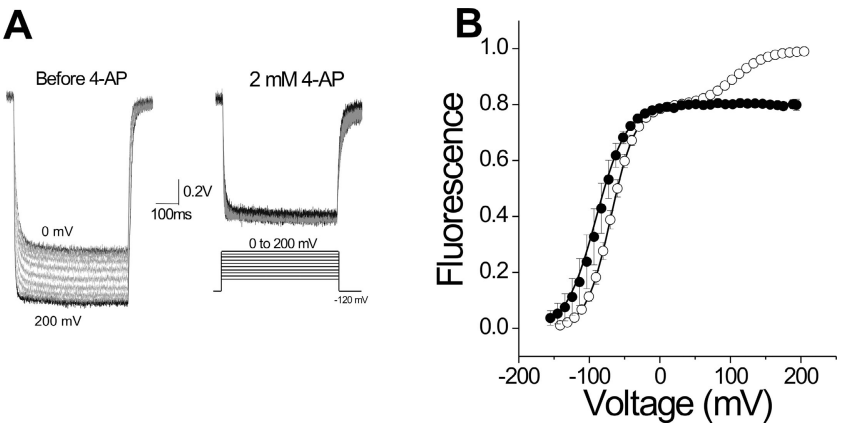

FIGURE 5. 4-AP eliminates the fluorescence change over the voltage range of opening for 359C-TMRM ILT. (A) Fluorescence changes for 359-TMRM ILT W434F channels from the same cell in the voltage range of opening in the absence (left) and presence (right) of 2 mM 4-AP added to the bath solution. Voltage protocol is shown as inset. (B) Steady-state fluorescence plotted as a function of voltage for channels in the absence of 4-AP (open circles) and in the presence of 2mM 4-AP (filled circles).

Gating Motion of S4 Is Associated with the Slow Inactivation Gates

Membrane depolarization not only opens the activation gate but also leads to slow inactivation by two distinct processes: P-type inactivation, which closes the outer end of the pore (De Biasi et al., 1993; Yang et al., 1997), and C-type inactivation, which shifts the voltage dependence of S4 motion (Olcese et al., 1997; Loots and Isacoff, 1998). These two forms of inactivation, originally referred to in the literature jointly as C-type inactivation (Timpe et al., 1988; Hoshi et al., 1991), appear to be mediated by the same gate, with P-type inactivation closing the slow inactivation gate and C-type inactivation stabilizing the gate's closed conformation and S4's activated conformation (Olcese et al., 1997; Yang et al., 1997; Loots and Isacoff, 1998). Earlier work on the related HERG potassium channel showed that the channel can undergo P-type inactivation without first opening its S6 gate (Smith and Yellen, 2002), indicating that the voltage sensor must be able to control the slow inactivation gate on its own. We wondered whether these two forms of slow inactivation are coupled to the activation motions of S4 or require S4 to undergo its final gating rearrangement. We approached this question by examining whether inactivation occurs from the activated state or the open state in the ILT channel.

P-type inactivation in ILT channels was tested in excised inside-out patches. On depolarization, ILT channels show a slow relaxation in current, which is affected by mutations at the external end of the selectivity filter. ILT channels carrying the mutation T449V, which is known to slow P-type inactivation (Lopez-Barneo et al., 1993), show a drastically slower relaxation compared with ILT channels (Fig. 6 A, i), indicating that the current relaxation is indeed due to inactivation. Under the ionic conditions used (MATERIALS AND METHODS), depolarization to +200 mV for 1 s produced an inactivation of ~35% (Fig. 6 A, ii). Following a 1-s depolarization to a specified voltage, a short step to a test potential of +200 mV was used to gauge the amount of P-type inactivation that took place during the prestep. We found P-type inactivation to occur only at positive voltages where channels open and not over the voltage range of activation. The voltage dependence of P-type inactivation intersected the G–V relation near its midpoint (Fig. 6 A, ii, right). This indicates that P-type inactivation does not proceed from the activated state of the channel, instead proceeding from the open state where S4 has undergone its final gating motion.

We next examined the voltage dependence of C-type inactivation. C-type inactivation can be monitored by measuring the shift in voltage dependence of either the gating charge movement or fluorescence report of S4-TMRM (Olcese et al., 1997; Loots and Isacoff, 1998). We used fluorescence measurements from TMRM attached to site 359 in channels carrying the W434F mutation. We used the W434F mutant because it strongly accelerates P-type inactivation (Yang et al., 1997; Loots and Isacoff, 1998), allowing us to follow the slower process of C-type inactivation. We compared F–Vs measured in response to two series of voltage steps: first from a holding potential of −80 mV and then from a holding potential of 0 mV. At −80 mV, most WT and ILT channels are at rest. As we have discussed above, at 0 mV, WT channels have undergone the gating motion of S4 and opened their S6 gate, while ILT channels are activated with their S6 gate closed. Agreeing with earlier observations (Loots and Isacoff, 1998), switching from a holding potential of −80 to 0 mV in WT channels produced a negative shift in the F–V that is the hallmark of C-type inactivation. However, no such shift was detected in ILT channels at 0 mV (Fig. 6 B), suggesting that the channels do not undergo C-type inactivation from the activated state. A trivial explanation for this observation could be that the ILT mutations render the channel incapable of C-type inactivation. This is difficult to test in the experimental configuration used due to the technical difficulty of holding a cell for long times at strong depolarizations (e.g., +100 mV to open ILT channels) in two-electrode voltage clamp. To test whether ILT

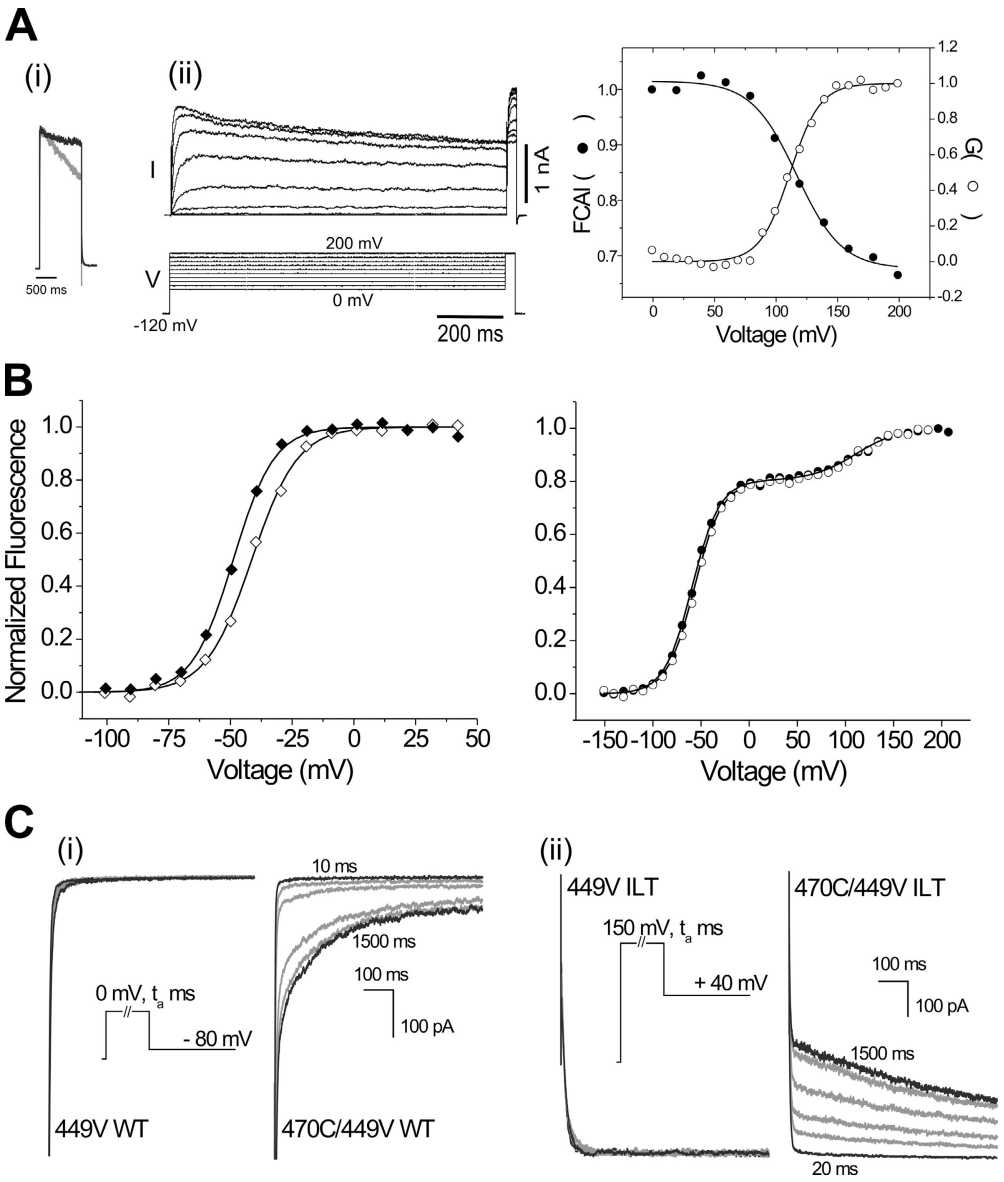

FIGURE 6. Slow inactivation in ILT channels over voltage range of S4's gating motion. (A, i) Superimposed currents in response to a 1-s depolarizing step to +150 mV for ILT channels (gray trace) and ILT/T449V channels (black trace) show that the T449V mutation slows slow inactivation of ILT channels. HP = −100 mV, post-step voltage = +40 mV. (ii) Voltage protocol (left, bottom) and currents (left, top) used for measuring the voltage dependence of slow (P-type) inactivation from conducting ILT channels in excised inside-out macropatches. Interval between sweeps = 5 s at an HP of −100 mV. The fraction of current after inactivation (FCAI, right, filled symbols) was plotted from the amplitude of the test pulse following the 1-s inactivating pulses after correcting for run-down in ionic current from patch (see MATERIALS AND METHODS). G–V for ILT channels measured from the same patch (right, open symbols). Data are representative of $n = 3$ patches. Solid lines are Boltzmann fits to the data. Fit parameters for data from three patches: for ILT Slow inactivation, $V_{1/2} = +108.6 \pm 9.8$ mV; G–V, $V_{1/2} = +101.4 \pm 6.9$ mV. (B) C-type inactivation does not occur from the activated state. Representative F–Vs for 359C WT W434F (left,) and 359C ILT W434F (right), from an HP of −80 mV (open symbols) or 0 mV (closed symbols). Interval between traces = 9 s. Solid lines represent single Boltzmann fits for WT and double Boltzmann fits for ILT. For 359C WT W434F, representative of $n = 3$: −80 mV hold, $V_{1/2} = -41.4$ mV, slope factor = 9.3; 0 mV hold, $V_{1/2} = -48.9$ mV, slope factor = 8.3. For 359C ILT W434F, representative of n = 4: double Boltzmann fit with −80 mV hold, $V1_{1/2} = -55.9$ mV, slope factor 1 = 14.0, $V2_{1/2} = +111.4$ mV, slope factor 2 = 20.5; 0 mV hold, $V1_{1/2} = -58.6$ mV, slope factor 1 = 14.1, $V2_{1/2} = +111.1$ mV, slope factor 2 = 23. (C) ILT channels undergo C-type inactivation. (i) Tail currents following a voltage step to 0 mV for 449V WT (left) and 470C/449V WT (right) channels. Voltage protocol is shown as inset; t_a is the duration of voltage step = 10, 40, 100, 400, 1,000, or 1,400 ms. (ii) Tail currents for 449V ILT and 470C/449V ILT channels following a voltage step to 150 mV with t_a = 20, 100, 200, 400, 1,000, or 1,500 ms. Recordings are from excised inside-out macropatches in symmetric (140 mM K^+) conditions. Tail current voltage for ILT channels is +40 mV since the inward tails at −80 mV are fast and hard to distinguish from the capacitive transient.

channels are capable of C-type inactivation, we used channels with the mutations T449V and I470C, measuring ionic current in the patch clamp configuration. The mutation 449V slows P-type inactivation, and the mutation 470C renders the C-type inactivated state conducting (Olcese et al., 2001). Thus, as observed earlier (Olcese et al., 2001), C-type inactivation in the 449V/470C Shaker IR channels can be followed by the appearance of an additional, slower deactivation component in tail currents following long depolarizations to a voltage where the channel is open (Fig. 6 C, i). When ILT channels carrying the 449V/470C mutations were opened by a depolarization to +150 mV, they showed the same slow deactivation component to the tail currents following long depolarizations as seen in WT channels that were opened by depolarization to 0 mV (Fig. 6 C, ii). As

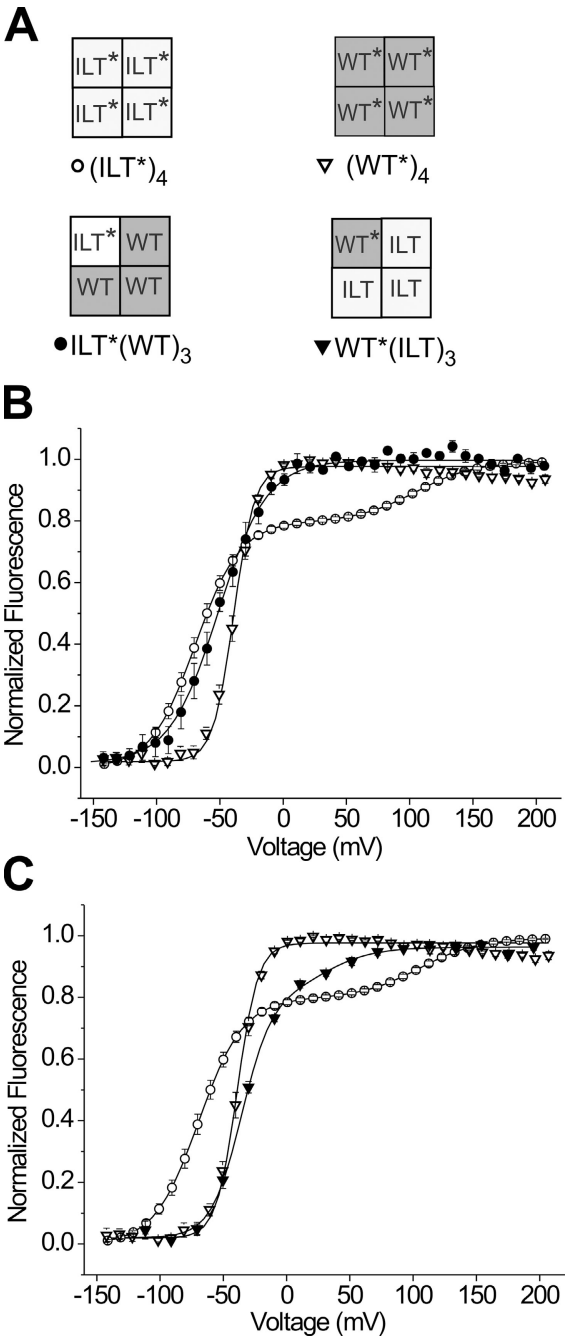

FIGURE 7. S4s move cooperatively over the voltage range that drives gating. (A) Subunit stoichiometry for hetero-tetrameric channels and their controls. * indicates a labeled subunit. Symbols shown under cartoons are same as used in graphs B and C. (B) Mean of F–Vs from labeled ILT*(WT)$_3$ (filled circles), (WT*)$_4$ (open, inverted triangles), and (ILT*)$_4$ channels (open circles). Solid lines are Boltzmann fits to the data. Fit parameters: ILT*(WT)$_3$ $V_{1/2}$ = −50.9 mV, slope factor = 19, n = 6; (WT*)$_4$ $V_{1/2}$ = −39.1 mV, slope factor = 8.2, n = 4. For (ILT*)$_4$, double Boltzmann fit parameters: $V1_{1/2}$ = −69.5 mV, slope factor = 17.6, $V2_{1/2}$ = +105.1 mV, slope factor = 23.3, n = 11. (C) Mean of F–Vs from labeled WT*(ILT)$_3$ (filled, inverted triangles). Fit parameters for WT*(ILT)$_3$ double Boltzmann fit $V1_{1/2}$ = −35.7 mV, slope factor = 12.0, $V2_{1/2}$ = 28.3 mV, slope factor = 20.5, n = 11; fits parameters to (WT*)$_4$ and (ILT*)$_4$ channels are same as in B.

in WT channels, this slower component of the tail current was not seen when the channel was opened by depolarization to the same voltage (+150 mV) for a shorter duration (e.g., 20 ms). These observations indicate that the ILT channel is capable of C-type inactivation from the open state of the channel where S4 has undergone its final gating motion. Taken together, these experiments on slow inactivation suggest that two forms of slow inactivation gating, P-type and C-type inactivation, are associated with the gating motion of S4.

Gating Motion of S4s Is Cooperative

The kinetic analysis of gating suggests that most of the charge moving steps of activation in Shaker channels occur mainly independently in each subunit, and that the ensuing opening steps of the channel are highly cooperative (Hoshi et al., 1994; Zagotta et al., 1994a,b; Schoppa and Sigworth, 1998a,b,c; Smith-Maxwell et al., 1998a). We earlier developed a method for monitoring cooperative interactions between subunits using single subunit fluorescence (Mannuzzu and Isacoff, 2000). Those previous experiments showed that the early activation phase is independent and that the late phase is cooperative, but were unable to distinguish between late activation steps and channel opening. We employed single subunit fluorescence to study cooperative interactions between the S4s of different subunits, taking advantage of the clean dissociation between the activation and gating motions of S4 in the ILT channel. We coinjected two different RNAs so as to favor the assembly of channels containing one labeled ILT subunit (359C ILT, designated as ILT*) with three unlabeled WT subunits (we refer to this heteromeric stoichiometry as ILT*(WT)$_3$). Alternatively, we examined mixed subunit channels in which RNA injection ratios favored one labeled WT subunit (359C WT, designated as WT*) to be coassembled with three unlabeled ILT subunits (this stoichiometry is referred to as WT*(ILT)$_3$) (Fig. 7 A). Our prediction was that if the S4 motions associated with activation and opening took place independently in each subunit, then the F–V of a labeled subunit should be the same regardless of whether it was combined with like subunits or different subunits. Deviation from this expectation would indicate cooperativity.

We found that in the voltage range of ILT activation, the F–V from ILT*(WT)$_3$ channels fell between the F–V of (ILT*)$_4$ channels and that of (WT*)$_4$, but much closer to (ILT*)$_4$ (Fig. 7 B). This suggests a weak influence of the WT subunits on the activation motion of the ILT subunit's S4. This is consistent with evidence supporting a mild cooperativity to the first of three otherwise independent charge-moving transitions of activation (Schoppa and Sigworth, 1998c). In contrast, at voltages more positive than −30 mV, the F–V of ILT*(WT)$_3$ closely tracked that of (WT*)$_4$, indicating a very strong influence of the three

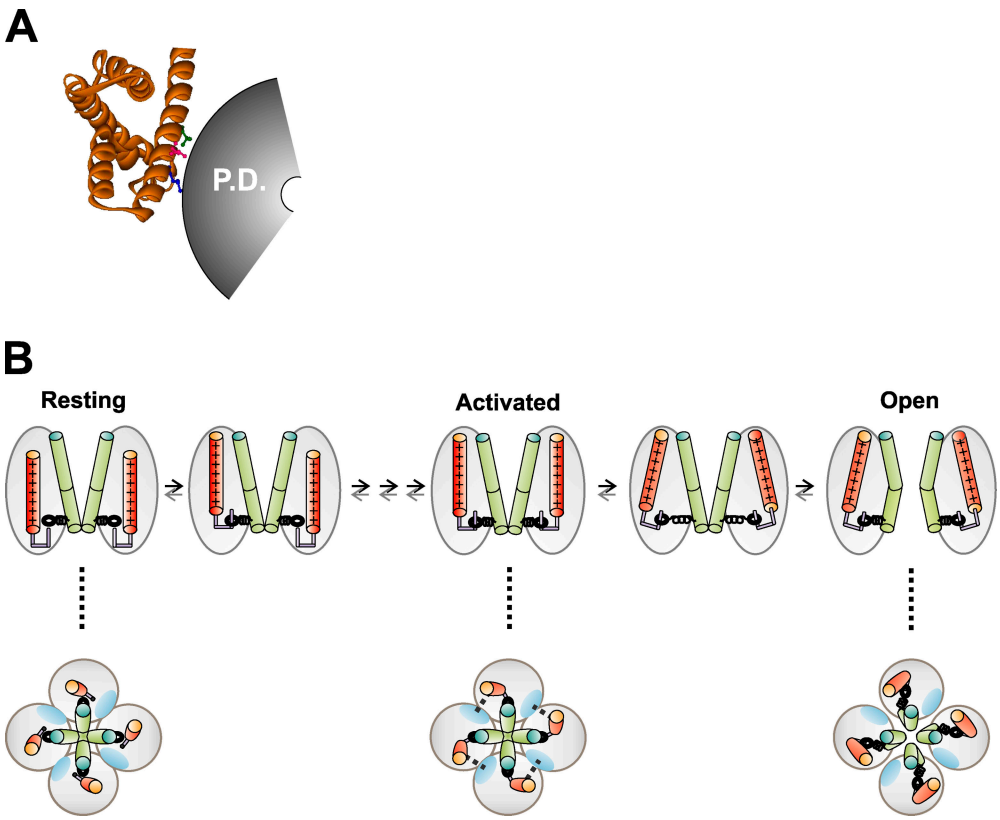

FIGURE 8. A model for channel opening. (A) Mapping of Shaker ILT positions onto the crystal structure of KvAP's isolated voltage sensing (S1–S4) domain (Jiang et al., 2003a) shows ILT residues to face away from other membrane segments in direction deduced to interact with the pore domain in the activated conformation (Gandhi et al., 2003). ILT residues are colored. P.D., pore domain. (B) Model for association between activation and gating motions of S4 and opening of the S6 gate. Top layer shows a side view of two subunits of the channel; dotted lines point to a top view of the channel with all four subunits shown. The S4s (orange cylinders) move independently (or with a mild cooperativity) of each other during activation, and do not exert force on the S6 gate (green cylinders). In the activated state, each S4 interacts with its neighboring S5 (blue oval, top view), which is denoted by dashed line. From the activated state, the S4s undergo a cooperative motion in which each S4 places strain on the S6 gate via S4–S5 (hook and spring representation). The interaction of an S4 with its neighboring S5 is stronger in ILT, hence a strong depolarization is needed to release S4 from its activated conformation to undergo its final motion.

WT subunits on the gating motion of the S4 of the ILT*. This is consistent with a proposed role of S4 in cooperativity (Smith-Maxwell et al., 1998a). Intersubunit influence was also greater for the opening step than for activation in heteromeric channels of the opposite stoichiometry. For WT*$(ILT)_3$ channels, the F–V from WT*$(ILT)_3$ overlapped that of $(WT^*)_4$ over the voltage range of activation, showing no influence of the ILT subunits on the activation motion of the WT subunit's S4 (Fig. 7 C). However, the F–V of WT*$(ILT)_3$ diverged considerably in the direction of $(ILT^*)_4$ over the voltage range of opening (Fig. 7 C). Thus, there is a strong intersubunit cooperativity in the gating motion of S4, and this is in contrast to the overall independence of the activation motions. The observation that three WT subunits make a single ILT subunit adopt an S4 gating motion that is so similar to WT suggests that the energy of three WT subunits is sufficient to open the channel.

DISCUSSION

One of the key puzzles of voltage-dependent gating is how the separate rearrangements of the four voltage sensors control the opening rearrangement of the S6 gate and closure of the slow inactivation gate in a coordinated manner. Earlier work has shown that activation involves a series of gating charge displacing steps mediated by successive outward motions of S4. Activation is followed by a cooperative channel opening step that itself displaces a small additional amount of gating charge (Schoppa and Sigworth, 1998c; Ledwell and Aldrich, 1999). Until now, the molecular basis of the gating charge displacement associated with opening was unclear (Patlak, 1999), but the ILT mutation has made it possible to probe opening in isolation from activation. Using ILT channels, we find that channel opening is accompanied by a final gating motion of S4. Two other gating processes, P-type and C-type slow inactivation, also appear to be linked to this S4 motion. The gating motion of S4 is found to be cooperative, in contrast to the preceding S4 motions of activation. Our results suggest that the S4s of a channel undergo two kinds of transmembrane motion: largely independent activation motions and a concerted or highly cooperative motion that could underlie the voltage dependence of the channel's final opening step.

In WT channels, the activation motions of S4 are tightly coupled to the cooperative S4 gating motion.

The ILT mutations disrupt this coupling, so that activation and opening occur with different rates and voltage dependence (Ledwell and Aldrich, 1999). How do three conservative point mutations (V369I, I372L, and S376T) bring about this effect? The ILT residues lie on one face of S4 (Fig. 8 A) and are buried in the span of the gating canal in the activated state (Larsson et al., 1996; Yusaf et al., 1996; Baker et al., 1998; Wang et al., 1999; Gandhi and Isacoff, 2002). The high impact of mutations on the ILT face of S4 on gating suggests that this face of S4 interacts with protein (Li-Smerin et al., 2000; Gandhi and Isacoff, 2002). Recent disulfide bonding and metal bridging studies indicate that this interaction is likely to be between the S4 in one subunit and the S5 of a neighboring subunit (Broomand et al., 2003; Gandhi et al., 2003; Laine et al., 2003; Neale et al., 2003). A strong intersubunit interaction between S4 and S5 could provide a physical basis for the cooperativity of the S4's gating motion and explain its special role in driving the gating rearrangements of the pore domain. The negative shift in the ILT channel's Q–V and positive shift in the G–V suggest that the three point mutations V369I, I372L, and S376T stabilize S4 in the activated state, thus requiring stronger depolarization to drive it through its final gating transition. This could be due to a stronger interaction between S4 and its neighboring S5 mediated through the ILT face of S4 (Fig. 8 B, bottom).

The normally tight coupling between the activation and gating motions of S4 is disrupted not only by the ILT mutation but also by mutations at L382 in the S4–S5 linker (Schoppa and Sigworth, 1998a,b,c). The similarity of the effects of these mutants implies that coupling depends on a combination of the gating motion of S4 and a rearrangement in the S4–S5 linker. A gating motion of S4 can drive such a rearrangement. An S4–S5 rearrangement may be key to pulling the internal end of S5 away from the central axis to allow the S6 gate to open (for example see Durell et al., 2004).

Our observations suggest that the activation motions of the S4s are permissive to gating, unlocking each subunit independently, without exerting force on the gates, and that a final concerted motion of all four S4s drives the S6 gate to open and the slow inactivation gate to close (Fig. 8 B). The cooperativity of the gating motion of S4, its relatively small charge displacement, and its tight coupling to gating suggest that this motion differs from the S4 motions of activation. We postulate that the final S4 motion has a smaller TM component and a larger lateral component than the activation motion. We conclude that S4 has two roles during membrane depolarization: (1) individual subunit motions that sense voltage and place all four S4s in an activated state, followed by (2) a concerted motion in all four S4s that applies force to the gates. This latter motion of S4 may be fundamental to gating in 6-TM channels as a class. The weak voltage dependence of this S4 gating motion can explain why some S4-containing channels (such as CNG channels and some SK channels) have a weak voltage dependence, while others, which also have the major transmembrane motions of S4, are steeply voltage dependent.

We would like to thank Rick Aldrich for the ILT construct, Lidia Mannuzzu and Eli Loots for guidance in the early part of this work, and Sandra Wiese for expert technical assistance. We are grateful to Richard Kramer for the use of his patch clamp setup, and would like to thank Chris Gandhi, Arnd Pralle, Harold Lecar, Richard Kramer, Pau Gorostiza, Michael Grabe, and members of the Isacoff laboratory for many helpful discussions and critical comments on the manuscript.

This work was funded by the National Institutes of Health, and a postdoctoral fellowship from the American Heart Association to F. Tombola.

Olaf S. Andersen served as editor.

Submitted: 21 October 2004
Accepted: 3 December 2004

REFERENCES

Aggarwal, S., and R. MacKinnon. 1996. Contribution of the S4 segment to gating charge in the Shaker K^+ channel. *Neuron.* 16: 1169–1177.

Ahern, C., and R. Horn. 2004. Specificity of charge-carrying residues in the voltage sensor of potassium channels. *J. Gen. Physiol.* 123:205–216.

Armstrong, C. 1969. Inactivation of the potassium conductance and related phenomena caused by quarternary ammonium ion injected into squid giant axons. *J. Gen. Physiol.* 54:533–575.

Baker, O., H. Larsson, L. Mannuzzu, and E. Isacoff. 1998. Three transmembrane conformations and sequence-dependent displacement of the S4 domain in shaker K^+ channel gating. *Neuron.* 20: 1283–1294.

Broomand, A., R. Mannikko, H.P. Larsson, and F. Elinder. 2003. Molecular movement of the voltage sensor in a K channel. *J. Gen. Physiol.* 122:741–748.

Cha, A., and F. Bezanilla. 1998. Structural implications of fluorescence quenching in the Shaker K^+ channel. *J. Gen. Physiol.* 112: 391–408.

Cha, A., G. Snyder, P. Selvin, and F. Bezanilla. 1999. Atomic scale movement of the voltage-sensing region in a potassium channel measured via spectroscopy. *Nature.* 402:809–813.

Chapman, M., H. VanDongen, and A. VanDongen. 1997. Activation-dependent subconductance levels in the drk1 K channel suggest a subunit basis for ion permeation and gating. *Biophys. J.* 72:708–719.

De Biasi, M., H.A. Hartmann, J.A. Drewe, M. Taglialatela, A.M. Brown, and G.E. Kirsch. 1993. Inactivation determined by a single site in K^+ pores. *Pflugers Arch.* 422:354–363.

Durell, S.R., I.H. Shrivastava, and H.R. Guy. 2004. Models of the structure and voltage-gating mechanism of the shaker K^+ channel. *Biophys. J.* 87:2116–2130.

Flynn, G., and W. Zagotta. 2001. Conformational changes in S6 coupled to the opening of cyclic nucleotide-gated channels. *Neuron.* 30:689–698.

Gandhi, C., E. Clark, E. Loots, A. Pralle, and E. Isacoff. 2003. The orientation and molecular movement of a K^+ channel voltage-sensing domain. *Neuron.* 40:515–525.

Gandhi, C., and E. Isacoff. 2002. Molecular models of voltage sensing. *J. Gen. Physiol.* 120:455–463.

Gandhi, C., E. Loots, and E. Isacoff. 2000. Reconstructing voltage sensor-pore interaction from a fluorescence scan of a voltage-gated K^+ channel. *Neuron.* 27:585–595.

Glauner, K., L. Mannuzzu, C. Gandhi, and E. Isacoff. 1999. Spectroscopic mapping of voltage sensor movement in the Shaker potassium channel. *Nature.* 402:813–817.

Holmgren, M., M. Jurman, and G. Yellen. 1996. N-type inactivation and the S4–S5 region of the Shaker K^+ channel. *J. Gen. Physiol.* 108:195–206.

Hoshi, T., W.N. Zagotta, and R.W. Aldrich. 1991. Two types of inactivation in Shaker K^+ channels: effects of alterations in the carboxy-terminal region. *Neuron.* 7:547–556.

Hoshi, T., W.N. Zagotta, and R.W. Aldrich. 1994. Shaker potassium channel gating. I: Transitions near the open state. *J. Gen. Physiol.* 103:249–278.

Isacoff, E., Y. Jan, and L. Jan. 1991. Putative receptor for the cytoplasmic inactivation gate in the Shaker K^+ channel. *Nature.* 353: 86–90.

Jiang, Y., A. Lee, J. Chen, M. Cadene, B. Chait, and R. MacKinnon. 2002a. Crystal structure and mechanism of a calcium-gated potassium channel. *Nature.* 417:515–522.

Jiang, Y., A. Lee, J. Chen, M. Cadene, B. Chait, and R. MacKinnon. 2002b. The open pore conformation of potassium channels. *Nature.* 417:523–526.

Jiang, Y., A. Lee, J. Chen, V. Ruta, M. Cadene, B. Chait, and R. MacKinnon. 2003a. X-ray structure of a voltage-dependent K^+ channel. *Nature.* 423:33–41.

Jiang, Y., V. Ruta, J. Chen, A. Lee, and R. MacKinnon. 2003b. The principle of gating charge movement in a voltage-dependent K^+ channel. *Nature.* 423:42–48.

Laine, M., M. Lin, J. Bannister, W. Silverman, A. Mock, B. Roux, and D. Papazian. 2003. Atomic proximity between S4 segment and pore domain in Shaker potassium channels. *Neuron.* 39:467–481.

Larsson, H., O. Baker, D. Dhillon, and E. Isacoff. 1996. Transmembrane movement of the shaker K^+ channel S4. *Neuron.* 16:387–397.

Lecar, H., H. Larsson, and M. Grabe. 2003. Electrostatic model of S4 motion in voltage-gated ion channels. *Biophys. J.* 85:2854–2864.

Ledwell, J., and R. Aldrich. 1999. Mutations in the S4 region isolate the final voltage-dependent cooperative step in potassium channel activation. *J. Gen. Physiol.* 113:389–414.

Li-Smerin, Y., D. Hackos, and K. Swartz. 2000. A localized interaction surface for voltage-sensing domains on the pore domain of a K^+ channel. *Neuron.* 25:411–423.

Liu, Y., M. Holmgren, M. Jurman, and G. Yellen. 1997. Gated access to the pore of a voltage-dependent K^+ channel. *Neuron.* 19:175–184.

Loboda, A., and C. Armstrong. 2001. Resolving the gating charge movement associated with late transitions in K channel activation. *Biophys. J.* 81:905–916.

Loots, E., and E. Isacoff. 1998. Protein rearrangements underlying slow inactivation of the Shaker K^+ channel. *J. Gen. Physiol.* 112: 377–389.

Loots, E., and E. Isacoff. 2000. Molecular coupling of S4 to a K^+ channel's slow inactivation gate. *J. Gen. Physiol.* 116:623–636.

Lopez-Barneo, J., T. Hoshi, S.H. Heinemann, and R.W. Aldrich. 1993. Effects of external cations and mutations in the pore region on C-type inactivation of Shaker potassium channels. *Receptors Channels.* 1:61–71.

Mannuzzu, L., and E. Isacoff. 2000. Independence and cooperativity in rearrangements of a potassium channel voltage sensor revealed by single subunit fluorescence. *J. Gen. Physiol.* 115:257–268.

Mannuzzu, L., M. Moronne, and E. Isacoff. 1996. Direct physical measure of conformational rearrangement underlying potassium channel gating. *Science.* 271:213–216.

McCormack, K., W. Joiner, and S. Heinemann. 1994. A characterization of the activating structural rearrangements in voltage-dependent Shaker K^+ channels. *Neuron.* 12:301–315.

Neale, E., D. Elliott, M. Hunter, and A. Sivaprasadarao. 2003. Evidence for inter-subunit interactions between S4 and S5 transmembrane segments of the shaker potassium channel. *J. Biol. Chem.* 278:29079–29085.

Olcese, R., R. Latorre, L. Toro, F. Bezanilla, and E. Stefani. 1997. Correlation between charge movement and ionic current during slow inactivation in Shaker K^+ channels. *J. Gen. Physiol.* 110:579–589.

Olcese, R., D. Sigg, R. Latorre, F. Bezanilla, and E. Stefani. 2001. A conducting state with properties of a slow inactivated state in a shaker K^+ channel mutant. *J. Gen. Physiol.* 117:149–163.

Patlak, J. 1999. Cooperating to unlock the voltage-dependent K channel. *J. Gen. Physiol.* 113:385–388.

Perozo, E., R. MacKinnon, F. Bezanilla, and E. Stefani. 1993. Gating currents from a nonconducting mutant reveal open-closed conformations in Shaker K^+ channels. *Neuron.* 11:353–358.

Sanguinetti, M., and Q. Xu. 1999. Mutations of the S4-S5 linker alter activation properties of HERG potassium channels expressed in *Xenopus* oocytes. *J. Physiol.* 514:667–675.

Schoppa, N., K. McCormack, M. Tanouye, and F. Sigworth. 1992. The size of gating charge in wild-type and mutant Shaker potassium channels. *Science.* 255:1712–1715.

Schoppa, N., and F. Sigworth. 1998a. Activation of shaker potassium channels. I. Characterization of voltage-dependent transitions. *J. Gen. Physiol.* 111:271–294.

Schoppa, N., and F. Sigworth. 1998b. Activation of Shaker potassium channels. II. Kinetics of the V2 mutant channel. *J. Gen. Physiol.* 111:295–311.

Schoppa, N., and F. Sigworth. 1998c. Activation of Shaker potassium channels. III. An activation gating model for wild-type and V2 mutant channels. *J. Gen. Physiol.* 111:313–342.

Seoh, S., D. Sigg, D. Papazian, and F. Bezanilla. 1996. Voltage-sensing residues in the S2 and S4 segments of the Shaker K^+ channel. *Neuron.* 16:1159–1167.

Smith, P.L., and G. Yellen. 2002. Fast and slow voltage sensor movements in HERG potassium channels. *J. Gen. Physiol.* 119:275–293.

Smith-Maxwell, C.J., J.L. Ledwell, and R.W. Aldrich. 1998a. Role of the S4 in cooperativity of voltage-dependent potassium channel activation. *J. Gen. Physiol.* 111:399–420.

Smith-Maxwell, C.J., J.L. Ledwell, and R.W. Aldrich. 1998b. Uncharged S4 residues and cooperativity in voltage-dependent potassium channel activation. *J. Gen. Physiol.* 111:421–439.

Stefani, E., L. Toro, E. Perozo, and F. Bezanilla. 1994. Gating of Shaker K^+ channels: I. Ionic and gating currents. *Biophys. J.* 66: 996–1010.

Timpe, L.C., Y.N. Jan, and L.Y. Jan. 1988. Four cDNA clones from the Shaker locus of *Drosophila* induce kinetically distinct A-type potassium currents in *Xenopus* oocytes. *Neuron.* 1:659–667.

Wang, M., S. Yusaf, D. Elliott, D. Wray, and A. Sivaprasadarao. 1999. Effect of cysteine substitutions on the topology of the S4 segment of the Shaker potassium channel: implications for molecular models of gating. *J. Physiol.* 521:315–326.

Webster, S., D. Del Camino, J. Dekker, and G. Yellen. 2004. Intracellular gate opening in Shaker K^+ channels defined by high-affinity metal bridges. *Nature.* 428:864–868.

Yang, N., A. George, and R. Horn. 1996. Molecular basis of charge movement in voltage-gated sodium channels. *Neuron.* 16:113–

122.

Yang, N., and R. Horn. 1995. Evidence for voltage-dependent S4 movement in sodium channels. *Neuron.* 15:213–218.

Yang, Y., Y. Yan, and F. Sigworth. 1997. How does the W434F mutation block current in Shaker potassium channels? *J. Gen. Physiol.* 109:779–789.

Yellen, G. 1998. The moving parts of voltage-gated ion channels. *Q. Rev. Biophys.* 31:239–295.

Yusaf, S., D. Wray, and A. Sivaprasadarao. 1996. Measurement of the movement of the S4 segment during the activation of a voltage-gated potassium channel. *Pflugers Arch.* 433:91–97.

Zagotta, W., T. Hoshi, and R. Aldrich. 1994a. Shaker potassium channel gating. III: Evaluation of kinetic models for activation. *J. Gen. Physiol.* 103:321–362.

Zagotta, W., T. Hoshi, J. Dittman, and R. Aldrich. 1994b. Shaker potassium channel gating. II: Transitions in the activation pathway. *J. Gen. Physiol.* 103:279–319.

Zheng, J., and F. Sigworth. 1998. Intermediate conductances during deactivation of heteromultimeric Shaker potassium channels. *J. Gen. Physiol.* 112:457–474.

Zheng, J., L. Vankataramanan, and F. Sigworth. 2001. Hidden Markov model analysis of intermediate gating steps associated with the pore gate of shaker potassium channels. *J. Gen. Physiol.* 118:547–564.